Laboratory Protocol

Characterization of Protein Stability, Catalysis and Aggregation

Molecular Biology and Biochemistry of Life
Winter Semester 2023-24

Authors
Masine Janet Tränkner
Syed Alisamar Husain

Supervisor
Dr. Titus M. Franzmann

Contents

List of Figures

Author Information

Masine Janet Tränkner
MSc. Computational Modelling and Simulation
Matriculation Number 5186813
masine_janet.traenkner@mailbox.tu-dresden.de

Syed Alisamar Husain
MSc. Computational Modelling and Simulation
Matriculation Number 5198172
syed_alisamar.husain@mailbox.tu-dresden.de

1 Temperature Induced Unfolding Transitions

The goal in this experiment is to determine the stability of the proteins Lysozyme and BSA (Bovine Serum Albumin) at different concentrations, 2.5, 5 and 10 µM, by inducing unfolding transitions through temperature changes. We detect unfolding using Fluorescence spectroscopy by measuring emission at two wavelengths, 330nm and 350nm, and we expect to see a sharp increase in the ratio of these emissions when the protein unfolds.

Measurements

The temperature was increased from 25 °C to 95 °C, at a rate of 2 °C per minute, and corresponding fluorescence at wavelengths 350nm and 330nm was measured.

- **Lysozyme - Fluorescence vs. Temperature**

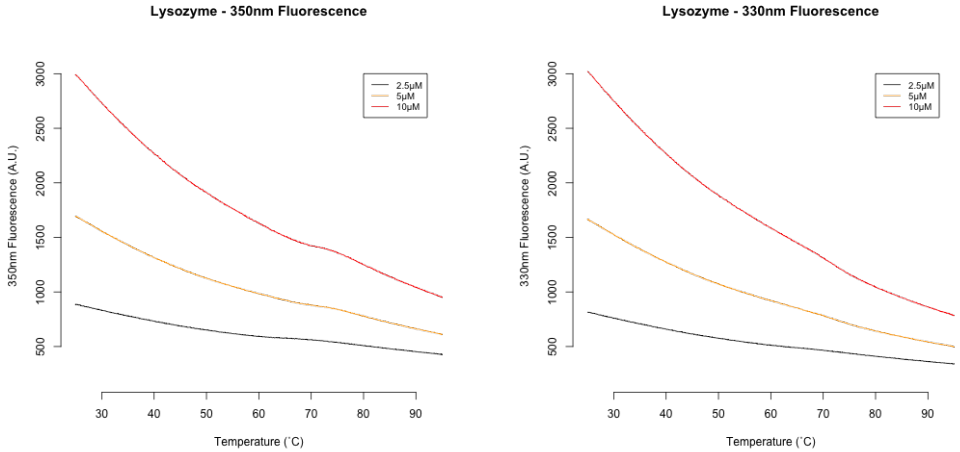

(a) (b)

Figure 1: Lysozyme Fluorescence at wavelengths (a) 350nm and (b) 330nm

- **BSA - Fluorescence vs. Temperature**

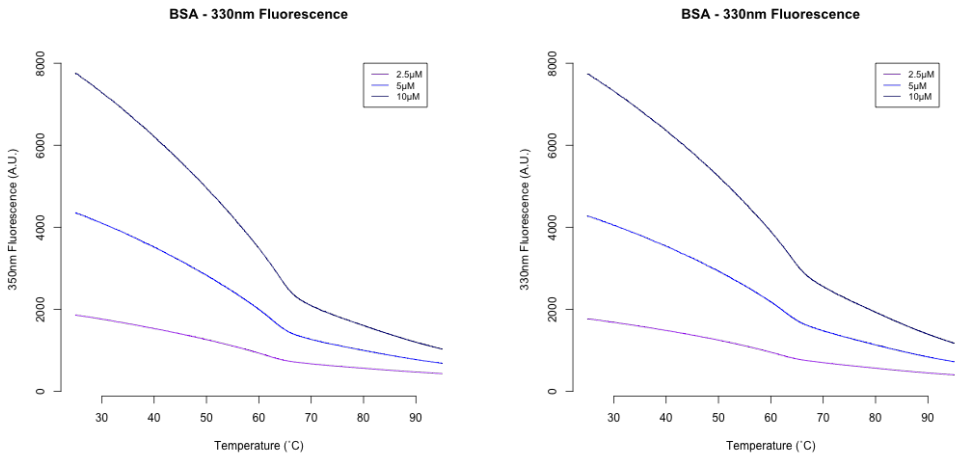

(a) (b)

Figure 2: BSA Fluorescence at wavelengths (a) 350nm and (b) 330nm

Analysis

The Fluorescence Ratio graph (Fig. 3(a) and Fig. 3(b)) was used to approximate the transition midpoint. Stability in the folded state arises from various interactions within the polypeptide. However, upon surpassing a threshold temperature, the polypeptide transitions to an unstable state. Consequently, as temperature increases, the population of unfolded molecules also rises. This process behaves differently for the two proteins.

For Lysozyme, a low ratio can be observed at the beginning, which indicates that the folded state predominates. With increasing temperature, this confirmation changes up to a threshold temperature and the transition of the molecules into the unfolded state, and accordingly the ratio also increases.

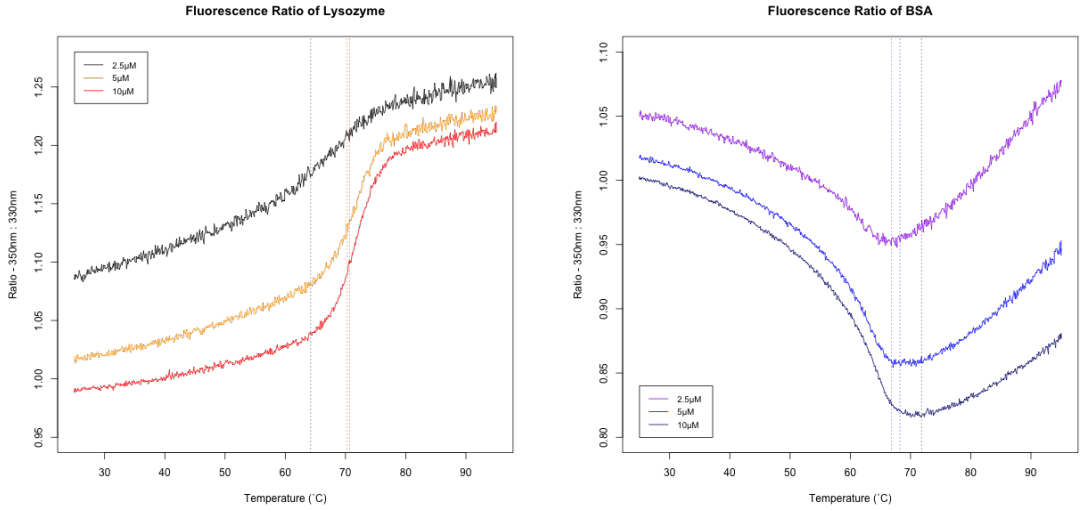

(a) (b)

Figure 3: Ratio of Fluorescence at 350nm to 330nm for (a) Lysozyme and (b) BSA

The opposite can be observed for BSA. Here, the ratio is already high at the start of the process and falls down to a certain threshold temperature. From this point, the ratio increases for all concentrations and thus also the amount of proteins in the unfolded state.

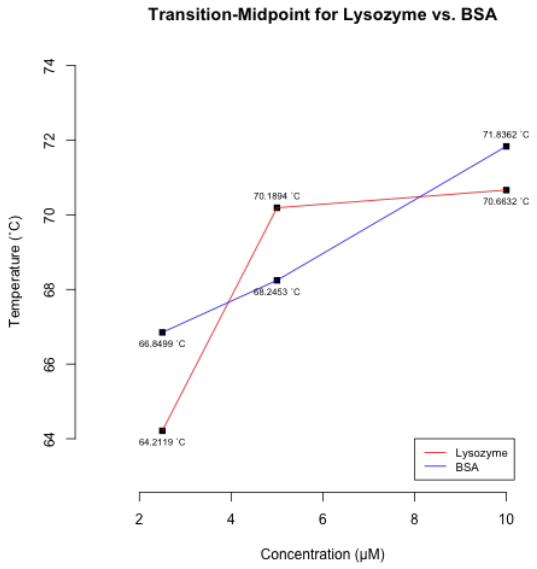

Figure 4: Ratio of Fluorescence at 350nm to 330nm for BSA

The transition midpoints relative to concentration are plotted in Figure 4. BSA shows a more linear temperature dependence than Lysozyme.

2 Lysozyme Aggregation Assay

In this experiment, aggregation of Lysozyme was studied to understand protein aggregation, where unfolded polypeptide chains of the proteins Lysozyme and Hsp27 associate irreversibly, leading to the formation of large particles that scatter light. Throughout the experiment, Hsp27 was used to analyze its effect on the aggregation of Lysozyme with presence of TCEP.

Measurements

Detecting the actual scattering of light is a challenging task that requires more equipment. Instead, we measure absorbance as a proxy for scattering using a pulsed spectrometer. We choose a wavelength which we know is not absorbed by anything in the mixture and we use that fact to say all of the intensity reduction is because of scattered light.

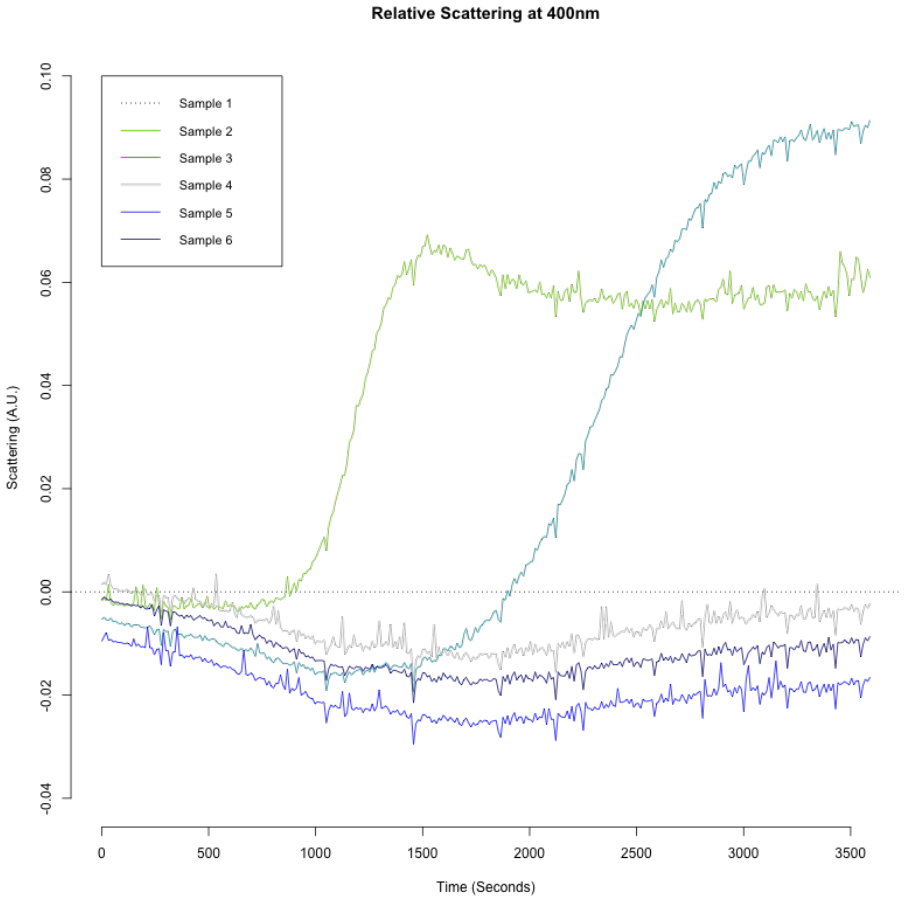

Figure 5: Scattering recorded as a function of time.

Analysis

As protein aggregation increases, more light is scattered by the sample. Introducing Hsp27 into the samples can regulate aggregation and consequently, scattering. At low concentrations of Hsp27 (Samples 1 to 3 in Figure 5), Lysozyme aggregation isn't effectively inhibited. Thus, the presence of Hsp27 in the solution increases overall absorption. But it can also be seen that a higher concentration of 10 µM (Sample 3) delays the aggregation.

However, when the concentration of Hsp27 matches that of Lysozyme, aggregation is prevented, resulting in lower absorbance (Sample 4). The control samples lacking Lysozyme and denaturant exhibit no absorbance change at 400nm (Samples 5 and 6). Only Samples 2 and 3 allow for the determination of an apparent halftime, which are $T_{50\%}^{S2} = 1200.30s$ and $T_{50\%}^{S3} = 2422.34s$ respectively, as their curves display a change of conformation.

3 Michaelis-Menten Kinetics

Lactatdehydrogenase (LDH) catalyzes the reaction conversion of Pyruvate into Lactate. In order to measure its activity the fluorescence of NADH, the cofactor of LDH, is measured under 340nm light. As NADH is converted to NAD^+, this fluorescence reduces and reaches a steady state when the reaction reaches equilibrium. We measure how fast this happens to determine the rate of reaction and find the Michaelis-Menten constants.

Measurements

We measure the absorbance of 340nm light through a sample of the reaction mixture over time and plot this in Figure 6. The slopes of these lines are directly proportional to the rates of reaction for each sample.

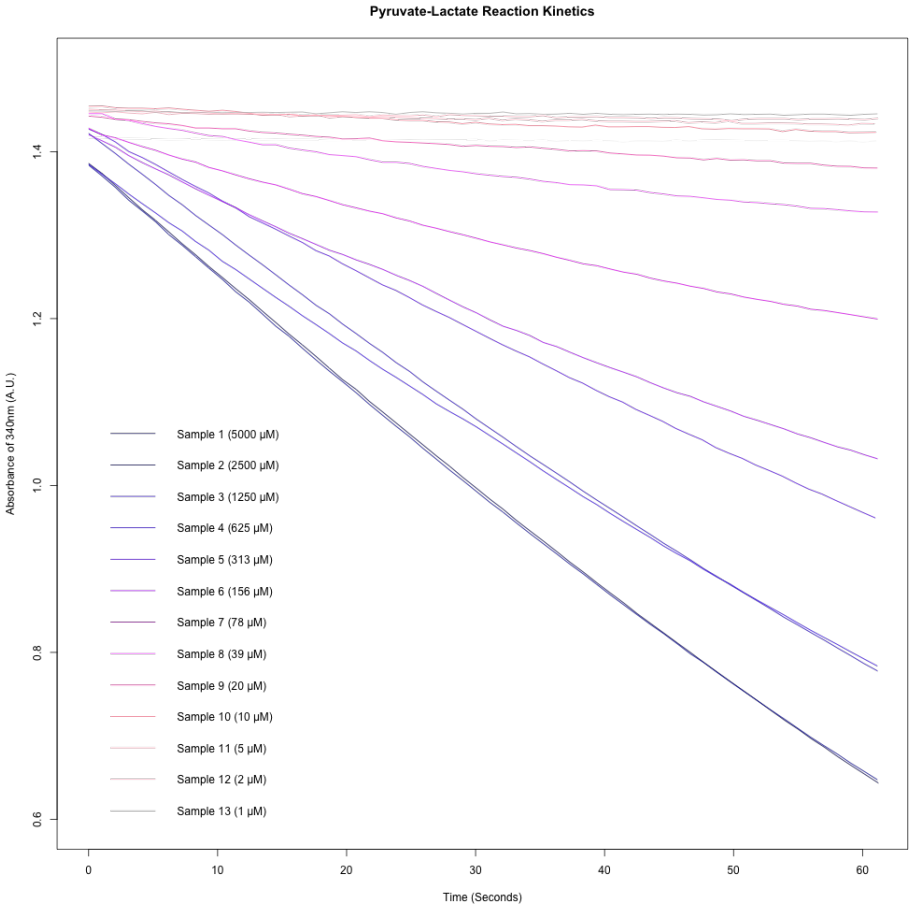

Figure 6: Absorbance as a function of time for different concentrations of Pyruvate

Analysis

The Michaelis-Menten plot (Fig. 7(a)) and the Lineweaver-Burk plot (Fig. 7(b)) can be plotted from reaction rates derived from change of absorbance over time, relative to the concentration of substrate. It is evident that for low substrate concentrations, the rate of the reaction increases linearly with increasing substrate concentration. As the substrate concentration increases, the rate of the reaction eventually reaches a maximum value (V_{max}). In this region, the active sites of the enzyme are largely occupied by the substrate, and the rate becomes independent of further increases in substrate concentration.

To find the maximum rate of reaction (V_{max}) and the Michaelis-Menten constant (K_m), we fit a linear model to the data, and the model estimates will give us an approximation of these constants.

The Michaelis-Menten equation $\frac{1}{V} = \frac{K_m}{V_{max}}\frac{1}{[S]} + \frac{1}{V_{max}}$ is of the form $y = \beta_1 x + \beta_0$.

Thus we have, $V_{max} = \frac{1}{\beta_0}$ and $K_m = \frac{\beta_1}{\beta_0}$

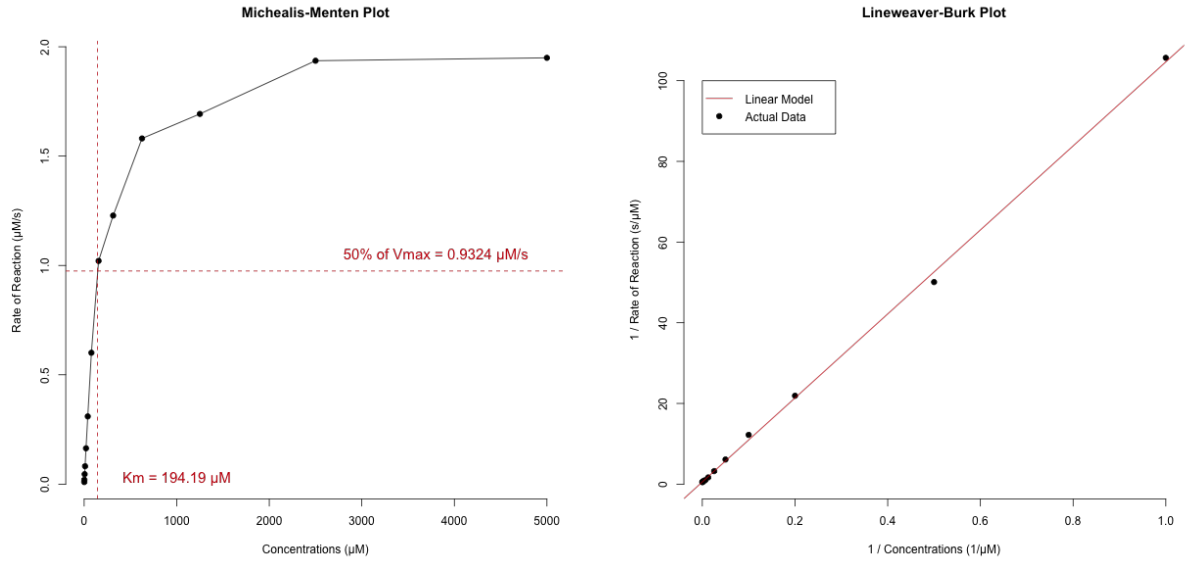

(a) (b)

Figure 7: Michaelis-Menten plot and Lineweaver-Burk plot

From the linear model estimates we get $V_{max} = 1.8649$ µM/s and for $K_m = 194.19$ µM. We mark the value $V_{max}/2$ on the Michaelis-Menten plot (Fig. 7(a)), which can also give us the value of K_m graphically. In the Lineweaver-Burk plot (Fig. 7(b)) the slope of the fitted line indicates the ratio $\frac{K_m}{V_{max}}$.

To find the change in NADH concentration for each sample, we can use the absorbance formula of Lambert-Beer, $A = \epsilon d C$, we have,

$$\Delta A = \epsilon d \Delta C.$$

Thus, $\Delta C = \frac{\Delta A}{\epsilon d}$, where $\epsilon = 6220 M^{-1} cm^{-1}$ and $d = 1$ cm

Thus, change in NADH concentration is calculated from the change in absorbance.

[Pyruvate] µM	ΔA (A.U.)	Δ[NADH] (µM)
5000	0.7425	119.3729
2500	0.7365	118.4083
1250	0.6441	103.5530
625	0.6013	96.67202
313	0.4660	74.91961
156	0.3884	62.44372
78	0.2286	36.75241
39	0.1179	18.95498
20	0.0623	10.01607
10	0.0311	4.999999
5	0.0173	2.781350
2	0.0076	1.221864
1	0.0036	0.578778

4 UV/VIS Spectroscopy of NADH

Similar to the kinetics experiment, the concentration should also be measured here using UV/VIS spectroscopy. The detected absorbance should show local maxima for 3 specific wavelengths (208, 260 and 340 nm). It is also to be expected that the absorbance also increases with increasing NADH concentration. However, according to figure x, the absorbance increases from sample 1 to 3, then increases for the samples 4 and 5 and again increases for sample 6, without exceeding the highest absorbance of sample 2.

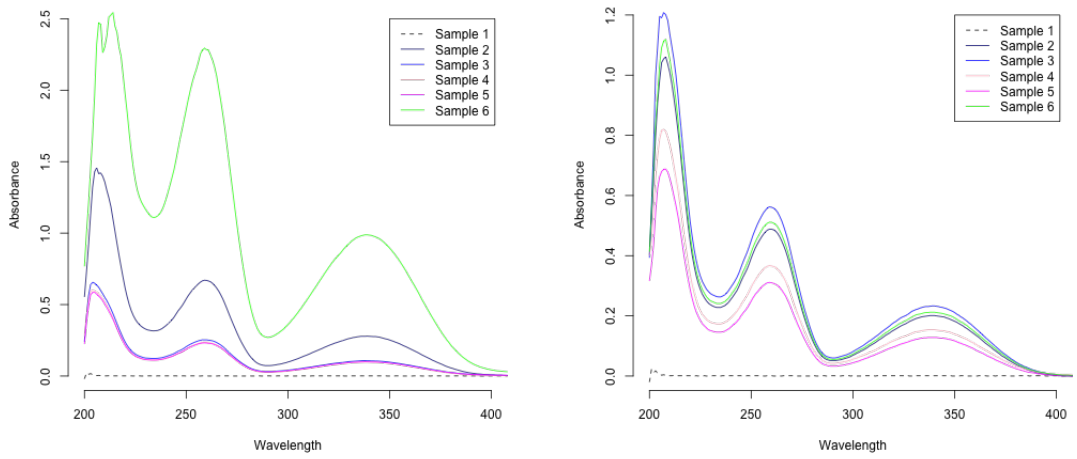

(Run 1) (Run 2)

Figure 8: Absorbance spectrum of NADH for different concentrations

Analysis

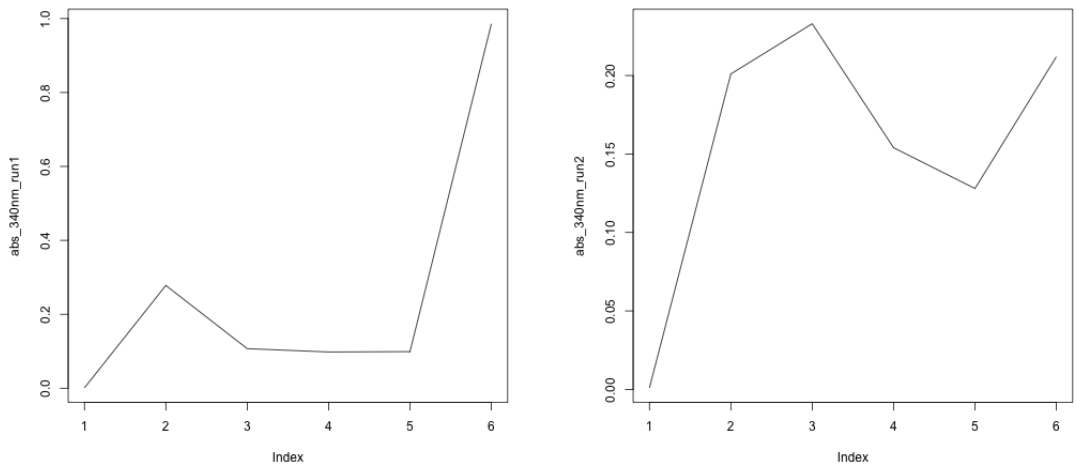

(Run 1) (Run 2)

Figure 9: Absorbance at 340nm for different concentrations